

Received 15 September 2022, accepted 13 October 2022, date of publication 17 November 2022,
date of current version 13 December 2022.

Digital Object Identifier 10.1109/ACCESS.2022.3223088

RESEARCH ARTICLE

Parallel Automatic Balance Control Method for the Magnetically Suspended Flywheel

LIMEI TIAN¹, YINGGUANG WANG, DENGYUN WU², JIYANG ZHANG, AND RUIZHI LUO

Beijing Institute of Control Engineering, Beijing 100190, China

Science and Technology on Space Intelligent Control Laboratory, Beijing 100190, China

Beijing Key Laboratory of Long-Life Technology of Precise Rotation and Transmission Mechanisms, Beijing 100194, China

Corresponding author: Yingguang Wang (wwangyingguang@126.com)

This work was supported by the National Natural Science Foundation of China under Grant 62173033.

ABSTRACT In order to attenuate the vibration caused by the radial imbalance in the Magnetically Suspended Flywheel (MSF), a parallel automatic balance control method is proposed. First, after the conduction of comparison between the parallel and series notch filter, a conclusion is drawn that the MSF achieves a better dynamic performance with greater attenuation on current vibration using the parallel notch filter. Then, experiments are performed under three conditions: without using the unbalance control, using radial unbalance control, and using axial unbalance control. The experimental results indicates that the stable automatic balance control and faster converging speed are achieved with the adoption of the proposed method. Furthermore, the vibration on the base is reduced significantly when the proposed method is introduced for all channels.

INDEX TERMS Magnetic bearing, magnetically suspended flywheel, vibration control, parallel notch filter.

I. INTRODUCTION

The inertial momentum wheel, acting as the spacecrafts attitude control actuator, has the advantages of no consumption on propellant and high output torque accuracy. It provides the accurate attitude control torque for spacecraft by regulating the rotor speed [1], [2], [3]. Suspended by the active magnetic bearings (AMBs), the magnetic suspended flywheel (MSF) has the advantage of high accuracy, long life, compact size, and low power consumption [4], [5]. Besides, owing to the closed-loop control, the base can avoid the influence from the rotor unbalanced vibration. Moreover, the drawback of zero-speed friction is absolutely overcome by the magnetic bearing, which presents much higher precision of attitude control. Thus, the MSF becomes an ideal attitude control actuator for spacecraft.

Because the implementation of magnetic control is based on the measured gap, the displacement measurement influenced by the rough surface causes the synchronous vibrations[6], [7]. In addition, the rotor mass imbalance can also attribute for the issues. Considering

that the vibration greatly influences the control precision, it becomes a research focus in the last decades, which can be divided into two categories. The two methods are used in different occasions related to the AMB-rotor systems.

One is the unbalance compensation control, which ensure the rotor to rotate around the geometric axis [8], [9], [10]. It is realized by compensating the unbalance force to achieve minimum displacement compensation. In [11], the unbalance compensation problem for AMB systems with input delays is investigated, and an unbalance compensation method is developed based on a solution to the output regulator problem for systems with input delay. Due to the difficulty arises in getting the correct estimations from unbalance responses alone, an algorithm based on the least-squares fit technique in frequency domain is used to identify the residual unbalances in flexible rotors at predefined balancing planes [12]. An adaptive unbalance compensation scheme is proposed in [13] based on the theory of immersion and invariance control. It estimates the information of mass imbalance online and is incorporated into the a stabilizing integral sliding mode controller so that the unbalance force can be eliminated.

The associate editor coordinating the review of this manuscript and approving it for publication was Laura Celentano³.

The other vibration control method is the automatic balance control, by the method of which the rotor rotates around the approximate inertial axis to minimize synchronous compensation force [14], [15], [16]. Since it is desired to minimize the base vibration from the rotor and avoid the power amplifier saturation caused by the excessive control current, the automatic balance control method is usually adopted. For example, Herzog et al. [17] proposed a generalized narrow-band notch filter, in which the parameters strongly depend on the inverse sensitivity matrix evaluated at rotational speed. Cui et al. [18] proposed an adaptive null vibration control method, which can remove the synchronous magnetic bearing force effectively, thus enabling the rotor rotate about its initial axis. In [19], a concise and direct explanation of the effects of notch filter on the rotor imbalance vibration with AMBs is proposed. The motion induced voltage due to the type of radial AMB was proven to be related with the synchronous vibration response. In the above research, the conventional notch filter or LMS algorithm is commonly used to achieve zero-current control, which series with the controller. However, the attenuation of the notch filter is not great enough, which limits the application. In addition, the conventional research is concentrated on the radial channel vibration suppress, in which the axial vibration is not considered. In this paper, the original of error introduced from axial displacement measurement is firstly analyzed. Based on the analysis, the axial automatic balance is proposed to eliminate the synchronous vibration force. At last, the effectiveness of the proposed method is verified by sufficient experiments.

II. MSF COMPONENTS AND MATHEMATICAL MODEL

As shown in Fig. 1, the MSF is composed of the following parts. 1) The rotor assembly including momentum wheel body, motor rotor and magnetic bearing. 2) The sealing cover and base providing the functions of safety protection, heat dissipation and sealing. 3) Magnetic bearing system including radial and axial magnetic bearing to realize the stable suspension control of the rotor with five degrees of freedom. The control system is composed of displacement sensors, controllers, and power amplifiers. 4) Motor system. The motor adopts an ironless BLDC motor. The rotor yoke is outside the motor stator, which is a type of inner rotor structure.

The electromagnetic force of the active magnetic bearing can be expressed as

$$f_x = f_+ - f_- = \frac{1}{4} \mu_0 n^2 A_a \left(\frac{(i_0 + i_x)^2}{(s_0 - x)^2} - \frac{(i_0 - i_x)^2}{(s_0 + x)^2} \right) \cos \alpha \quad (1)$$

where i_0 is the bias current; s_0 is the unilateral air gap length; x is the rotor displacement offset; α is the angle between the electromagnet and the shaft; μ_0 is the vacuum permeability; n is the number of coils, and A_a is the magnetic bearing pole area.

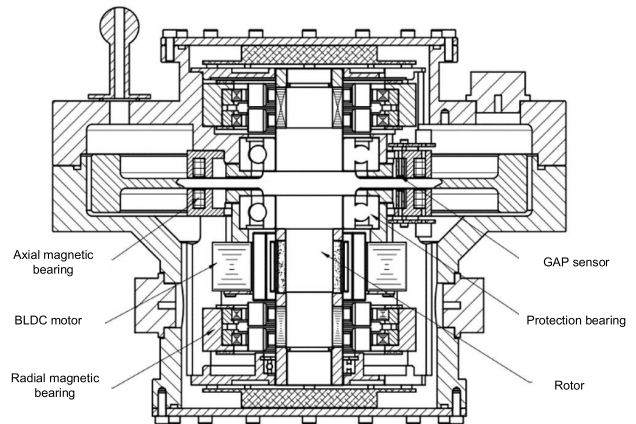


FIGURE 1. Structure of MSF.

Considering that $x \ll s_0$ is satisfied, (1) can be linearized as

$$f_x = \frac{4ki_0}{s_0^2} (\cos \alpha) i_x + \frac{4ki_0^2}{s_0^3} (\cos \alpha) x = k_i i_x - k_s x \quad (2)$$

where k_i and k_s are the force/current coefficient and force/displacement coefficient, respectively.

III. POSITION ERROR ANALYSIS ON AXIAL SENSOR MEASUREMENT SURFACE

Fed by the measured displacement, the control system generates magnetic force to suspend the rotor. Considering that the eddy current displacement sensor with small size of sensor probe is used, the performance of the magnetic suspension rotor system is easily influenced. Therefore, amount of interference signal is caused by geometric errors, and kinds of control algorithms are employed for the compensation. Although the rotor has been dynamically balanced off-line using the dynamic balancing machine, there is tiny residual imbalance left due to the accuracy limitation. In summary, the rotor imbalance mass and the deviation from the measuring surface to the displacement sensor result in the synchronous frequency interference. Then, the displacement sensor error in the axial direction causes vibration on the rotor and reduces the operating accuracy.

Owing to the adoption of the inner rotor type momentum wheel structure, the axial sensor cannot directly detect the position of the rotor shaft center. Thus, the displacement sensor probe is installed on side of the rotor for the size limitation. Due to the residual imbalance and unavoidable errors during the assembly process, the perpendicularity between the axial displacement measurement surface and the rotor rotation axis cannot be fully guaranteed.

The displacements from the geometric axis and the inertial axis of the rotor in the generalized coordinate can be respectively expressed as

$$\begin{aligned} \mathbf{q}_G &= [x_G, \beta_G, y_G, -\alpha_G]^T. \\ \mathbf{q}_I &= [x_I, \beta_I, y_I, -\alpha_I]^T. \end{aligned} \quad (3)$$

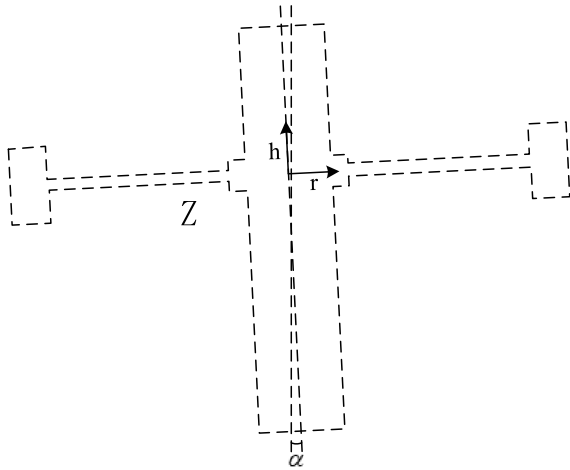


FIGURE 2. Rotor displacement of Z axis.

In the generalized coordinate system, the rotor imbalance is defined as

$$\Delta q = q_I - q_G = \begin{bmatrix} \varepsilon \cos(\Omega t + \chi) \\ \sigma \sin(\Omega t + \delta) \\ \varepsilon \sin(\Omega t + \chi) \\ -\sigma \cos(\Omega t + \delta) \end{bmatrix}. \quad (5)$$

The displacement sensor signal is assumed as $q_s = [s_{ax}, s_{bx}, s_{ay}, s_{by}]$. Based on the relationship between the generalized coordinate system and sensor coordinate system, q_s can be deduced as

$$q_s = T_s q_G = T_s (q_I - \Delta q) \quad (6)$$

where $T_s = k_s \begin{bmatrix} 1 & l_s & 0 & 0 \\ 1 & -l_s & 0 & 0 \\ 0 & 0 & 1 & l_s \\ 0 & 0 & 1 & -l_s \end{bmatrix}$, and k_s denotes the amplitude factor.

Considering the axial sensor probe and the X-direction sensor probe are installed on the same plane, the direction displacement is obtained as

$$r = \frac{s_{ax} + s_{bx}}{2} = s_x = x_I - \varepsilon \cos(\Omega t + \chi). \quad (7)$$

As shown in Fig.2, h denotes the axial displacement of the rotor, and the axial displacement sensor Z is located at the lower end of rotor. α denotes the angle between the axial rotor displacement measurement surface and the horizontal direction.

Thus, the output signal of the axial sensor can be described as

$$z = h \cdot \cos \alpha - r \cdot \sin \alpha. \quad (8)$$

Substituting (7) into equation (8) gives the displacement from axial sensor as

$$z = h \cdot \cos \alpha - [x_I - \varepsilon \cos(\Omega t + \chi)] \cdot \sin \alpha. \quad (9)$$

Therefore, from (9), the axial displacement sensor signal contains radial coupling interference, and the dynamic behavior of the rotor axis is influenced by radial unbalance.

Because the high machining accuracy is adopted, the rotor axial displacement measuring surface and the horizontal plane are simultaneously controlled in the rotor axis. Therefore, the rotor is controlled stably in five degrees of freedom. The rotor radially revolves around the inertial main shaft, and the magnetic bearing axial controller will not respond at the synchronous frequency. In addition, the axial force with the synchronous frequency will not be transmitted to the base, and the decouple of each DOF is realized.

IV. AUTOMATIC BALANCE CONTROL

The basic idea of automatic balance control is to eliminate the synchronous frequency in the displacement signal using the notch filter. With the elimination of the unbalanced disturbance in the displacement signal, the synchronous magnetic force is not generated. Therefore, the base vibration caused by synchronous disturbance will be significantly reduced. The automatic balance control is beneficial to reduce the reaction force at synchronous frequency, the consumed control energy, and the burden of the controller.

Based on the analysis above, a parallel adaptive notch filter for the automatic balance control is proposed. Taking the X_A channel as an example, as shown in Fig. 3, the notch filter $N_f(s)$ center frequency varies with the speed. The feedback coefficient ε determines the convergence speed and bandwidth of the notch filter.

Assuming that $x_f(t)$ and $c_f(t)$ are the input and output signals of $N_f(s)$, respectively. $c_f(t)$ can be expressed as

$$c_f(t) = [\sin \Omega t \quad \cos \Omega t] \begin{bmatrix} \int \sin \Omega t \cdot x_f(t) dt \\ \int \cos \Omega t \cdot x_f(t) dt \end{bmatrix} \quad (10)$$

where $c_f(t)$ and Ω satisfy the following equation

$$\ddot{c}_f(t) + \Omega^2 c_f(t) = \dot{x}_f(t). \quad (11)$$

Then the transfer function of the notch filter is written as

$$N_f(s) = \frac{c_f(s)}{x_f(s)} = \frac{s}{s^2 + \Omega^2}. \quad (12)$$

When the same frequency current control current is not introduced. The transfer function from u to i_{ax} can be deduced as

$$G_{ui}(s) = \frac{i_{ax}}{u} = -\frac{G_w(s)G_c(s)k_{ad}k_s}{1 + G_w(s)G_c(s)G_p(s)k_{ad}k_s}. \quad (13)$$

As shown in Fig. 2, in the parallel mode, the transfer function from u to i_{ax} can be denoted as

$$G'_{ui}(s) = \frac{i_{ax}}{u} = -\frac{G_w(s) \frac{G_c(s)}{1 + G_c(s)\varepsilon N_f(s)} k_{ad}k_s}{1 + \frac{G_w(s)G_c(s)}{1 + G_c(s)\varepsilon N_f(s)} G_p(s)k_{ad}k_s}. \quad (14)$$

Subtracting (12) into 14 gives

$$G'_{ui}(s) = \frac{i_{ax}}{u} = -\frac{G_w(s) \frac{(s^2 + \Omega^2)G_c(s)}{(s^2 + \Omega^2) + \varepsilon s G_c(s)} k_{ad}k_s}{1 + \frac{(s^2 + \Omega^2)G_w(s)G_c(s)}{(s^2 + \Omega^2) + \varepsilon s G_c(s)} G_p(s)k_{ad}k_s}. \quad (15)$$

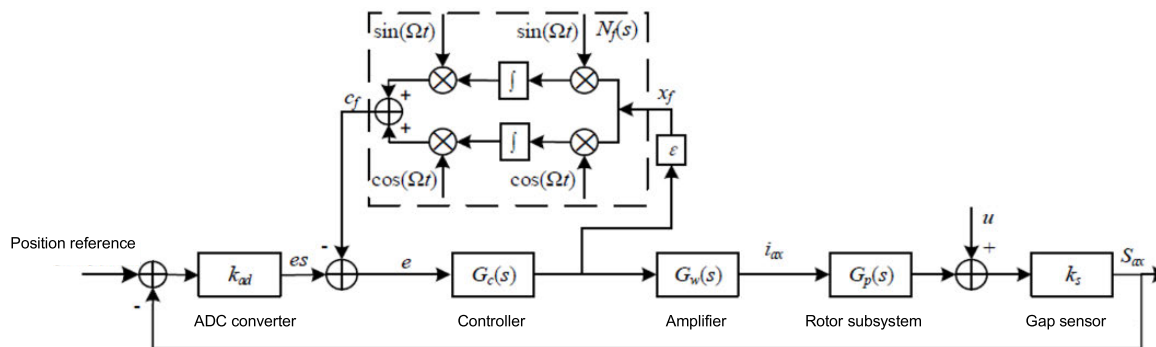


FIGURE 3. Parallel adaptive notch filter.

TABLE 1. Parameters of the MSF.

Parameter	Symbol	Unit	Value
Rotor mass	m	kg	4.7
Transverse moments of inertia	J_p	kg.m ²	0.031
Polar moments of inertia	J_d	kg.m ²	0.019
Distance from O to bearing center	l	mm	40
Maximum speed	f	Hz	100
Position stiffness	k_x	N · x ⁻¹	123.9
Current stiffness	k_i	N · A ⁻¹	333500

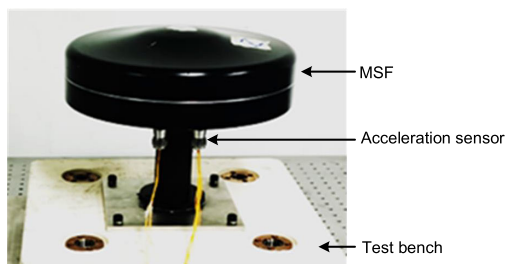


FIGURE 4. Experimental configuration of MSF.

Considering that the deviation part is a tiny value, which denotes as

$$\begin{cases} G'_{ui}(j\omega) \approx 0, & \omega \in (\Omega - \Delta\Omega, \Omega + \Delta\Omega) \\ G'_{ui}(j\omega) \approx G_{ui}(j\omega), & \omega \in (0, \Omega - \Delta\Omega) \cup [\Omega + \Delta\Omega, +\infty) \end{cases} \quad (16)$$

From the (16), the control current is equal to zero at Ω . But the frequency characteristics from the unbalanced amount to the control current has not changed at other frequencies.

V. EXPERIMENTAL RESULTS

As shown in Fig. 4, an experimental configuration is set up to verify the suppression effect of the axial automatic balance control. The maximum speed of the MSF rotor is 100 Hz. The parameters are shown in Table 1.

The test bench is a type of KISTLER-Z21492. Based on the analysis above, the experiments are divided into the following three different conditions.

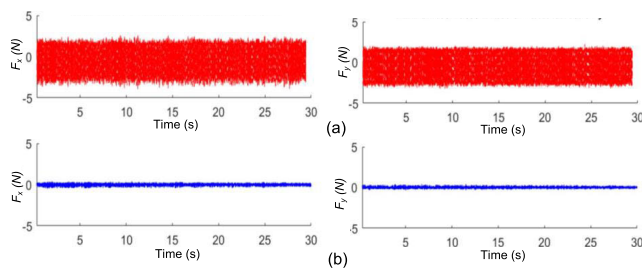


FIGURE 5. Radial force vibration comparison before and after the introduction of the proposed method. (a) Magnetic force variation before introducing the proposed method. (b) Magnetic force variation after introducing the proposed method.

1) With the unbalance control switched off, the rotor operates in a stable state only using the PID control method. Then, the base vibration during the rotor speed increasing is measured.

2) With the unbalance control switched on at the radial direction, the rotor is stably suspended. Then, the base vibration is measured during the acceleration of the MSF rotor speed.

3) With the unbalance control switched on in all channels, and the base vibration of the MSF is measured during the rotor acceleration.

As shown in Fig. 5, the radial vibration frequency spectrum of the base is compared before and after the introduction of proposed method at 30 Hz. The radial synchronous frequency vibration force of the base is large before the introduction of the proposed method. The output torque accuracy is seriously deteriorated. When the radial unbalance control is switched on, the radial synchronous frequency vibration of the base is greatly eliminated, which indicates that the proposed method presents an ideal performance.

After the employment of the automatic balance and unbalance control in the radial direction, the rotor speed continues to be controlled to increase. When the speed reaches 50 Hz, the amplitude of the axial synchronous frequency vibration of the base increases significantly, which results in larger oscillations in the axial direction. Then, imbalance

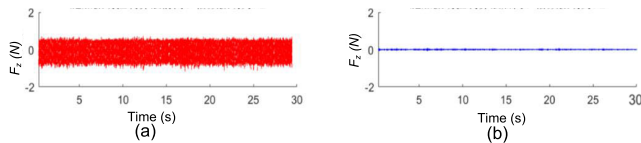


FIGURE 6. Axial force vibration comparison. (a) Magnetic force variation before introducing the proposed method. (b) Magnetic force variation after introducing the proposed method.

algorithm is activated in the axial direction. Fig. 6 shows the axial vibration frequency spectrum of the base before and after the introduction of the axial imbalance compensation control at 50 Hz. The synchronous frequency vibration of the base is weakened obviously, and the amplitude of the axial synchronous frequency vibration is reduced by about 80%.

In summary, the experimental results indicates that the simultaneous introduction of the axial and radial directions can suppress the synchronous frequency vibration of the base effectively, which greatly improves the stability of the system and realizes the “super static” operation.

VI. CONCLUSION

In this paper, it is firstly analyzed that the amplitude of the synchronous frequency vibration of the MSF base is determined by two factors. One is the rotor unbalanced mass, and the other is measured signal variation from the measuring surface to the displacement sensor. Then, based on the analysis, a parallel balance control method is proposed to reduce the axial vibration. Three different experiments are conducted, which cover the conditions of not switching on the balance control, only switching on radial unbalance control, and switching on the radial and axial unbalance control at the same time.

From the experiment, it is verified that radial and axial unbalance control switched on simultaneously presents a good performance on the attenuation of base vibration. In addition, it is proved that automatic balance control can also be achieved in the axial direction. Compared with the method only using the radial automatic balance control, the unbalance automatic balance control method achieved better performance, the application area of which has been broadened.

REFERENCES

- [1] H. Krishnan, N. H. McClamroch, and M. Reyhanoglu, “Attitude stabilization of a rigid spacecraft using two momentum wheel actuators,” *AIAA J. Guid. Contr. Dyn.*, vol. 18, no. 2, pp. 256–263, Apr. 1995.
- [2] Y.-K. Chang, B.-H. Lee, and S.-J. Kim, “Momentum wheel start-up method for HAUSAT-2 ultra-small satellite,” *Aerosp. Sci. Technol.*, vol. 10, no. 2, pp. 168–174, Mar. 2006.
- [3] L. Zhu, J. Guo, and E. Gill, “Review of reaction spheres for spacecraft attitude control,” *Prog. Aerosp. Sci.*, vol. 91, pp. 67–86, May 2017.
- [4] X. Chen, Y. Ren, Y. Cai, J. Chen, W. Wang, and X.-D. Yang, “Spacecraft vibration control based on extended modal decoupling of Vernier-gimballing magnetically suspension flywheels,” *IEEE Trans. Ind. Electron.*, vol. 67, no. 5, pp. 4066–4076, Jan. 2019.

- [5] G. B. Gallego, L. Rossini, E. Onillon, T. Achtnich, C. Zwyssig, R. Seiler, D. M. Araujo, and Y. Perriard, “On-line micro-vibration measurement method for Lorentz-type magnetic-bearing space actuators,” *Mechatronics*, vol. 64, Dec. 2019, Art. no. 102283.
- [6] K. Wang, X. Ma, Q. Liu, S. Chen, and X. Liu, “Multiphysics global design and experiment of the electric machine with a flexible rotor supported by active magnetic bearing,” *IEEE/ASME Trans. Mechatronics*, vol. 24, no. 2, pp. 820–831, Apr. 2019.
- [7] S. Zheng, X. Liu, Y. Zhang, B. Han, Y. Shi, and J. Xie, “Temperature drift compensation for exponential hysteresis characteristics of high-temperature eddy current displacement sensors,” *IEEE Sensors J.*, vol. 19, no. 23, pp. 11041–11049, Aug. 2019.
- [8] M. Meng, Y. H. Fan, and J. Y. Zhang, “Micro-vibration characteristics and its adaptive vibration control of magnetically suspended flywheels,” *Aerosp. Control Appl.*, vol. 40, no. 2, pp. 53–58, 2014.
- [9] X. Huang and Z. Tang, “New method for auto balancing with active magnetic bearings,” *Chin. J. Mech. Eng.*, vol. 37, no. 7, pp. 96–99, 2001.
- [10] X. Wang, Z. Deng, and S. Zhao, “Study on unbalance compensation for rotor of magnet suspension based on optimal control,” *Electro-Mech. Eng.*, vol. 24, no. 4, pp. 61–64, 2008.
- [11] S. Y. Yoon, L. Di, and Z. Lin, “Unbalance compensation for AMB systems with input delay: An output regulation approach,” *Control Eng. Pract.*, vol. 46, pp. 166–175, Jan. 2016.
- [12] R. Tiwari and A. Chougale, “Identification of bearing dynamic parameters and unbalance states in a flexible rotor system fully levitated on active magnetic bearings,” *Mechatronics*, vol. 24, no. 3, pp. 274–286, Feb. 2014.
- [13] S.-L. Chen, S.-Y. Lin, and C.-S. Toh, “Adaptive unbalance compensation for a three-pole active magnetic bearing system,” *IEEE Trans. Ind. Electron.*, vol. 67, no. 3, pp. 2097–2106, Mar. 2020.
- [14] H. G. Chiacchiarini and P. S. Mandolesi, “Unbalance compensation for active magnetic bearings using ILC,” in *Proc. IEEE Int. Conf. Control Appl.*, Mexico City, Mexico, Sep. 2001, pp. 58–63.
- [15] A. L. Matras, G. T. Flowers, R. Fuentes, M. Balas, and J. Fausz, “Suppression of persistent rotor vibrations using adaptive techniques,” *J. Vibrot. Acoust.*, vol. 128, no. 6, pp. 682–689, Dec. 2006.
- [16] C. Hui, L. Shi, J. Wang, and S. Yu, “Adaptive unbalance vibration control of active magnetic bearing systems for the HTR-10GT,” in *Proc. 18th Int. Conf. Nucl. Eng.*, Xi’an, China, 2010, pp. 1–9.
- [17] R. Herzog, P. Buhler, C. Gahler, and R. Larssonneur, “Unbalance compensation using generalized notch filters in the multivariable feedback of magnetic bearings,” *IEEE Trans. Control Syst. Technol.*, vol. 4, no. 5, pp. 580–586, Sep. 1996.
- [18] P. Cui, J. He, and J. Fang, “Static mass imbalance identification and vibration control for rotor of magnetically suspended control moment gyro with active-passive magnetic bearings,” *J. Vibrot. Control*, vol. 22, no. 10, pp. 2313–2334, Jun. 2014.
- [19] J. Zhou, S. Zheng, B. Han, and J. Fang, “Effects of notch filters on imbalance rejection with heteropolar and homopolar magnetic bearings in a 30-kW 60 000-r/min motor,” *IEEE Trans. Ind. Electron.*, vol. 64, no. 10, pp. 8033–8041, Apr. 2017.



LIMEI TIAN received the B.S. degree in detection technology and automation and the M.S. degree in measuring and testing technologies and instruments from Beihang University, Beijing, China, in 2002 and 2005, respectively. She is currently a Research Fellow with the Beijing Institute of Control Engineering. Her research interests include high precision servo control, spacecraft actuator, vibration control of flywheels suspended by magnetic bearings, and fault diagnosis.



YINGGUANG WANG received the B.S. degree in industrial automation from Shandong University, Weihai, China, in 2006, and the Ph.D. degree in precision instruments and machinery from Beihang University, Beijing, China, in 2014.

He is currently an Engineer with the Beijing Institute of Control Engineering, Beijing. His research interests include theoretical and experimental analysis of magnetic levitation devices, novel inertial instrument and equipment technology, and vibration control of flywheels suspended by magnetic bearings.



JIYANG ZHANG received the Ph.D. degree from the School of Instrumentation and Optoelectronic Engineering, Beihang University, Beijing, China.

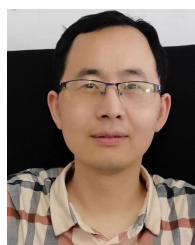
He is currently serving as a Research Fellow with the Beijing Institute of Control Engineering, Beijing. His research interests include spacecraft attitude control and actuator design.



DENGYUN WU received the B.S. degree from the Taiyuan University of Technology, Taiyuan, China, in 1997, the M.S. degree from Southeast University, Nanjing, China, in 2002, and the Ph.D. degree from the Harbin Institute of Technology, Harbin, China, in 2021.

He is currently an Engineer and a Research Fellow with the Beijing Institute of Control Engineering, Beijing, China. His research interests include theoretical and experimental analysis of

magnetic levitation devices, novel inertial instrument and equipment technology, vibration control of flywheels suspended by magnetic bearings, high precision servo control, spacecraft actuator, vibration control of mechanical systems, and fault diagnosis.



RUIZHI LUO received the Ph.D. degree from the China Academy of Space Technology. He is currently a Research Fellow with the Beijing Institute of Control Engineering. His research interests include high precision servo control and vibration control for spacecraft actuator.

...